Supplemental Materials for "Factors controlling variability in the oxidative capacity of the troposphere since the Last Glacial Maximum," Evaluation of present-day ICECAP simulation

L. T. Murray*[1], L. J. Mickley[1], J. O. Kaplan[2], E. D. Sofen[3], M. Pfeiffer[2], and B. Alexander[3]

[1]School of Engineering an2ed Applied Sciences, Harvard University, Cambridge, MA, USA
[2]ARVE Group, École Polytechnique Fédérale de Lausanne, Lausanne, Switzerland
[3]Department of Atmospheric Sciences, University of Washington, Seattle, WA, USA
*Now at: Lamont-Doherty Earth Observatory, Columbia University, Palisades, NY, USA

1 Description of simulations used for evaluation

The main text introduces the model framework for ICE age Chemistry And Proxies (ICECAP), a project focused on paleo-chemistry at and since the Last Glacial Maximum. The framework includes the GEOS-Chem 3-D global chemical transport model (CTM; http://www.geos-chem.org), driven by archived meteorology from the NASA Goddard Institute for Space Sciences (GISS) ModelE general circulation model (GCM). Here we evaluate the performance of the present-day ModelE-driven simulation versus a standard suite of observations used to test chemical and physical processes (e.g., transport, convection, and wet deposition). We also compare our results with state-of-the-science GEOS-Chem simulations driven by two different assimilated meteorological products from the Goddard Earth Observing System (GEOS) of the NASA Global Modeling and Assimilation Office. The GEOS4 product consists of 6 h means for most fields and 3 h means for surface fields, with a horizontal resolution of 1 latitude by 1.25 longitude and with 55 layers in the vertical. The GEOS5 product (version 5.1.0) has the same temporal resolution as GEOS4 and a horizontal resolution of 0.5 latitude by 0.667 longitude with 72 layers in the vertical. For this evaluation, the GEOS4 and GEOS5 products are upscaled to 4 latitude by 5 longitude, and to 30 and 47 vertical layers, respectively.

1.1 SF_6 simulation

Sulfur hexafluoride (SF_6) is a trace gas of industrial origin that is chemically and physically inert on human time scales, with an atmospheric lifetime of 3200 years (Maiss and Brenninkmeijer, 1998). It is emitted primarily over industrialized regions of the northern hemisphere, and its meridional gradient is a useful test for meridional mixing (Rigby et al., 2010; Hall et al., 2011). It is also used with other long-lived gases to infer mean age of air in the stratosphere (Waugh and Hall, 2002). We perform three 43-year simulations of SF_6 in GEOS-Chem, each using a single year of present-day ModelE,

*ltmurray@post.harvard.edu

GEOS4 (1993), and GEOS5 (2005) meteorology and emissions from the Emissions Database for Global Atmospheric Research (EDGAR) version 4.0 (http://edgar.jrc.ec.europa.eu, 2009) for 1970-2012.

1.2 Radionuclide simulation

Radon-222, lead-210, and beryllium-7 comprise the standard set of radionuclides used for evaluation of global atmospheric chemistry and climate models.

Terrigenic ^{222}Rn is an inert, insoluble, short-lived (half-life 3.8 d) noble gas produced from the slow decay of ^{226}Ra (half-life 1600 a) found in uranium ores. Its evasion from surface soils is relatively uniform and constant, but reduced when the surface is frozen. Its insolubility and time scale of decay make it a useful tracer for diagnosing quick vertical mixing within atmospheric models from moist convection and boundary layer mixing and ventilation (e.g., Allen et al., 1996; Brost and Chatfield, 1989; Considine et al., 2005; Feichter and Crutzen, 1990; Hauglustaine et al., 2004; Jacob, 1990; Jacob et al., 1997; Lambert et al., 1982; Mahowald et al., 1995; Stockwell et al., 1998).

Table 1: Global budgets of radionuclides in GEOS-Chem simulations using different meteorology [a]

		GEOS4	GEOS5	ModelE
Rn-222				
Global Burden, g		193	192	188
Troposphere		193 (99.8%)	192 (99.8%)	188 (100.%)
Stratosphere		0.43 (0.2%)	0.45 (0.2%)	0.02 (0.0%)
Tropospheric residence time, d		5.5	5.5	5.5
Sources, g d^{-1}		35	35	34
Sinks, g d^{-1}		35	35	34
Pb-210				
Global Burden, g		323	383	257
Troposphere		285 (88%)	322 (84%)	216 (84%)
Stratosphere		38 (12%)	61 (16%)	41 (16%)
Tropospheric residence time, d		8.6	9.7	6.7
Sources, g d^{-1}		33	33	32
Sinks, g d^{-1}		33	33	32
Radioactive Decay	Tropospheric	0.02 (0%)	0.03 (0%)	0.02 (0%)
	Stratospheric	0 (0%)	0.01 (0%)	0 (0%)
Dry Deposition		4 (11%)	3 (11%)	2 (7%)
Wet Deposition	Stratiform	10 (30%)	10 (31%)	12 (36%)
	Convective	20 (59%)	19 (59%)	18 (56%)
Be-7				
Global Burden, g		16	16	15
Troposphere		3.8 (25%)	4.4 (27%)	5.5 (36%)
Stratosphere		11.7 (75%)	12 (73%)	9.6 (64%)
Tropospheric residence time, d		21.1	24.8	25.7
Sources, g d^{-1}		0.33	0.33	0.33
Cosmogenic	Tropospheric	0.14 (41%)	0.13 (40%)	0.15 (44%)
	Stratospheric	0.2 (59%)	0.2 (60%)	0.19 (56%)
Sinks, g d^{-1}		0.33	0.33	0.34
Radioactive Decay	Tropospheric	0.05 (15%)	0.06 (17%)	0.07 (21%)
	Stratospheric	0.15 (46%)	0.16 (47%)	0.13 (37%)
Dry Deposition		0.01 (3%)	0.01 (3%)	0 (1%)
Wet Deposition	Stratiform	0.04 (12%)	0.04 (11%)	0.04 (12%)
	Convective	0.08 (24%)	0.07 (22%)	0.1 (29%)

[a] Parentheses give percentage of total global burden, source, or sink

Radiogenic ^{210}Pb is the chemically-inert decay daughter of ^{222}Rn. It is readily taken up by submicron aerosol particles and subsequently removed from the atmosphere by deposition or decay (Bondietti et al., 1988; Maenhaut

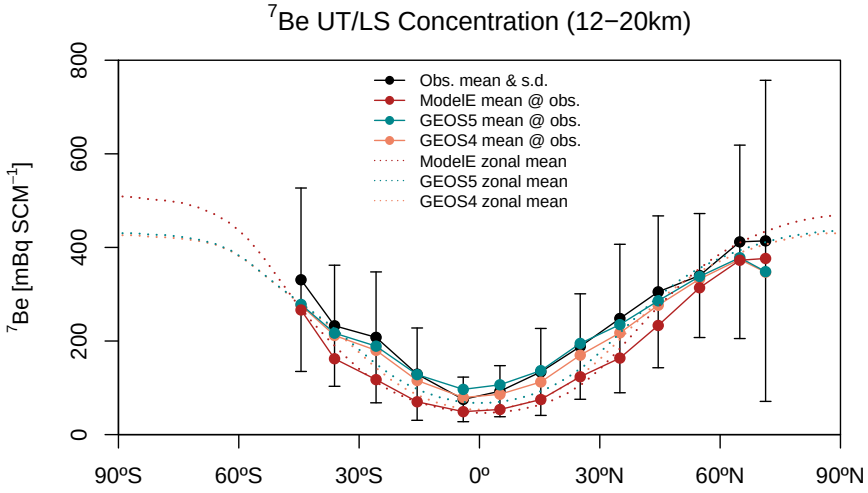

Figure 1: Comparison of model ^{7}Be source parameterization with UT/LS aircraft observations from the DOE RAdioNuclide DAtaBase (RANDAB) from 1957-1983. The data are from the Oak Ridge National Laboratory Carbon Dioxide Information Analysis Center (http://cdiac.ornl.gov/; doi: 10.3334/CDIAC/atg.db1019) and have been linearly adjusted for solar activity using Usoskin et al. (2005).

et al., 1979; Preiss et al., 1996; Sanak et al., 1981). Because of its relatively long lifetime (half-life 22.2 a), nearly all ^{210}Pb is removed via deposition. As its source from ^{222}Rn is relatively well known and there exists a global and long-term surface deposition flux and concentration inventory (Preiss et al., 1996), it is the standard test for modeled wet deposition. The source of ^{210}Pb is evaluated in Section 2.3.

Cosmogenic ^{7}Be is produced by the cosmic ray spallation of N_2 and O_2, predominantly in the polar upper troposphere and lower stratosphere (UT/LS) (Lal et al., 1958). Like ^{210}Pb, it is rapidly taken up by submicron aerosol particles (Bondietti et al., 1988; Maenhaut et al., 1979; Papastefanou, 2009; Papastefanou and Ioannidou, 1996; Sanak et al., 1981). It is subsequently transported until removal by rainout or surface deposition in the troposphere, or by radioactive decay (half-life 53.3 d). ^{7}Be has been used to constrain vertical transport, wet deposition fluxes, and stratosphere-troposphere exchange (STE) in models (e.g., Allen et al., 2003; Brost et al., 1991; Koch et al., 1996; Liu et al., 2001, in prep.; Barrett et al., 2012).

Table 1 gives the atmospheric budget of simulations in GEOS-Chem of these three radionuclides driven by meteorology from ModelE (4 years of present-day meteorology), and the GEOS4 (2004-2006) and GEOS5 (2004-2006) assimilated products. Emissions of ^{222}Rn within GEOS-Chem are those of Jacob et al. (1997). We simulate the source of ^{7}Be using the parameterization of Usoskin and Kovaltsov (2008) for mean solar activity, which leads to an average production of 0.064 atoms cm ^{2} s ^{1}; about 60% in the stratosphere and 40% in the troposphere. Figure 1 evaluates the source of ^{7}Be in the model by showing concentrations of UT/LS ^{7}Be in the model versus aircraft observations for 1957-1983 from the Department of Energy RAdioNuclide DAtaBase (RANDAB). The model distributions match those of the RANDAB dataset (R^2 = 0.48-0.53). In the the region of greatest production, the extratropical lower stratosphere, the models are all biased low by 10-13% relative to the observations, although well within the range of observed variability.

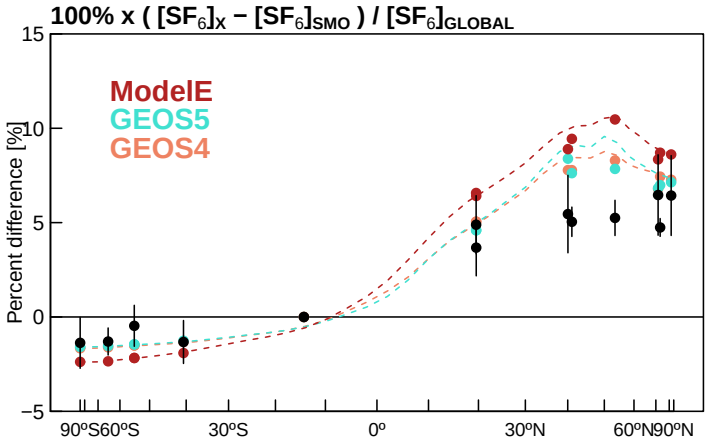

Figure 2: Meridional gradient of SF_6 in flask samples for 1995-2005 at 13 flask sites in the NOAA Earth System Research Laboratory (ESRL) Global Monitoring Division (GMD; http://www.esrl.noaa.gov/gmd). All values are shown as percent differences relative to American Samoa (SMO). Vertical bars show the standard deviation in the observations. Also shown are the values from the CTM driven by different meteorology products, sampled at the observations (filled circles), and the zonal mean (dashed lines).

1.3 Full chemistry simulation

We also analyze the present-day ozone-NO_x-CO-VOC-BrO_x-aerosol simulation as described in the main text driven by ModelE (using three years of 1990s meteorology) and GEOS4 meteorology (1994-1996). Both simulations have identical anthropogenic emissions. We use identical treatment of natural emissions, and modify the standard GEOS4 simulation to be consistent with the ModelE-driven simulation (e.g., lightning uses a global NO_x yield per flash, and is not constrained to satellite observations). Total emissions and their distribution therefore differ with the different meteorology.

2 Evaluation

2.1 Horizontal Mixing

Figure 2 shows the observed meridional gradient of SF_6 in monthly mean flask samples of surface air from NOAA, relative to the concentration at American Samoa (SMO) in the remote tropical southern Pacific. Also shown is each simulation sampled as in the observations, and the zonal mean gradient. In all simulations, GEOS-Chem overestimates the meridional gradient in SF_6 by 60-100%. This suggests that the inter-hemispheric mixing rate in the model is too slow, and/or that the EDGAR inventory overestimates the emissions growth rate in the northern hemisphere relative to the southern hemisphere. However, the difference between the ModelE and GEOS simulations with identical emissions indicates that GEOS-Chem driven by ModelE has about a 25% slower rate of meridional mixing than by the GEOS simulations.

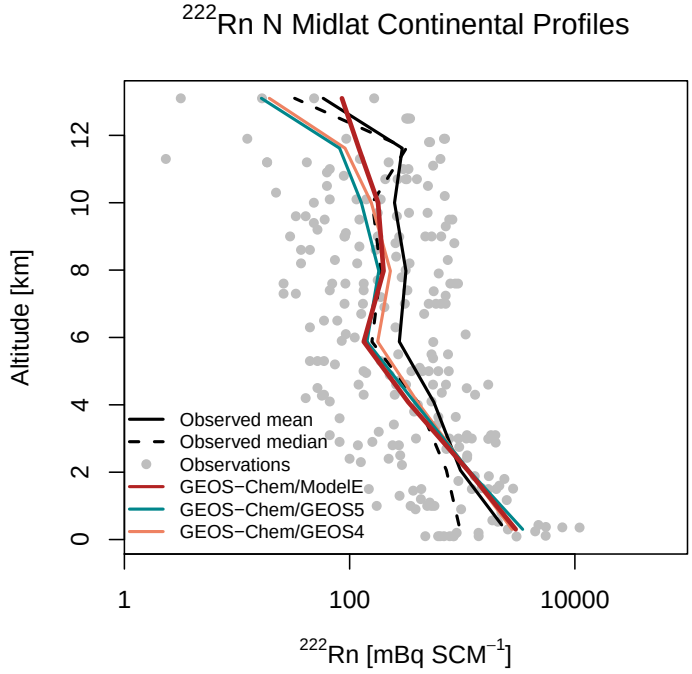

Figure 3: Mean observed vertical profile of ^{222}Rn compared with GEOS-Chem sampled at month and location of observations (Bradley and Pearson, 1970; Nazarov et al., 1970; Wilkening, 1970; Moore et al., 1973; Kritz et al., 1998). The units are mBq per standard cubic meter at 0 C and 1 atm, calculated with a linear transformation of the molar mixing ratio (5.637 mBq SCM ^{1} = 1.0 $\times 10^{22}$ mol ^{222}Rn / mol air).

2.2 Vertical Mixing

2.2.1 Troposphere

We assess vertical mixing within the troposphere using vertical profiles of ^{222}Rn, and ratios of ^{7}Be/^{210}Pb in surface air.

Figure 3 shows simulated climatological ^{222}Rn profiles sampled at the month and location of available observations, also plotted. Observations are scarce and available only at northern extratropical continental locations. In an overly-convective atmosphere, the vertical gradient of ^{222}Rn would disappear. In all of our simulations, there is a slight overestimate within the boundary layer and underestimate above, implying a small underestimate in boundary layer ventilation. Our results are comparable to or better than other CTMs/GCMs (e.g., Considine et al., 2005). All three simulations represent the climatological median of the measurements well, especially above the boundary layer. ModelE reproduces the ^{222}Rn distribution the best of the three models (ModelE R^2 = 0.46; GEOS5 = 0.34; GEOS4 = 0.42), particularly in the upper troposphere.

Figure 4 shows the annual mean surface concentration of ^{7}Be simulated with mean solar activity, surface ^{210}Pb, and their ratio. Given the difference in the source regions for the two molecules, and that the ratio of ^{7}Be/^{210}Pb is unaffected by deposition, the ratio serves as a useful measure of vertical mixing in the troposphere (Koch et al., 1996). A persistent high bias would indicate excessive downward transport and/or insufficient upward transport, assuming no bias in either source. The filled circles represent measurements from surface monitoring stations of the DOE Environ-

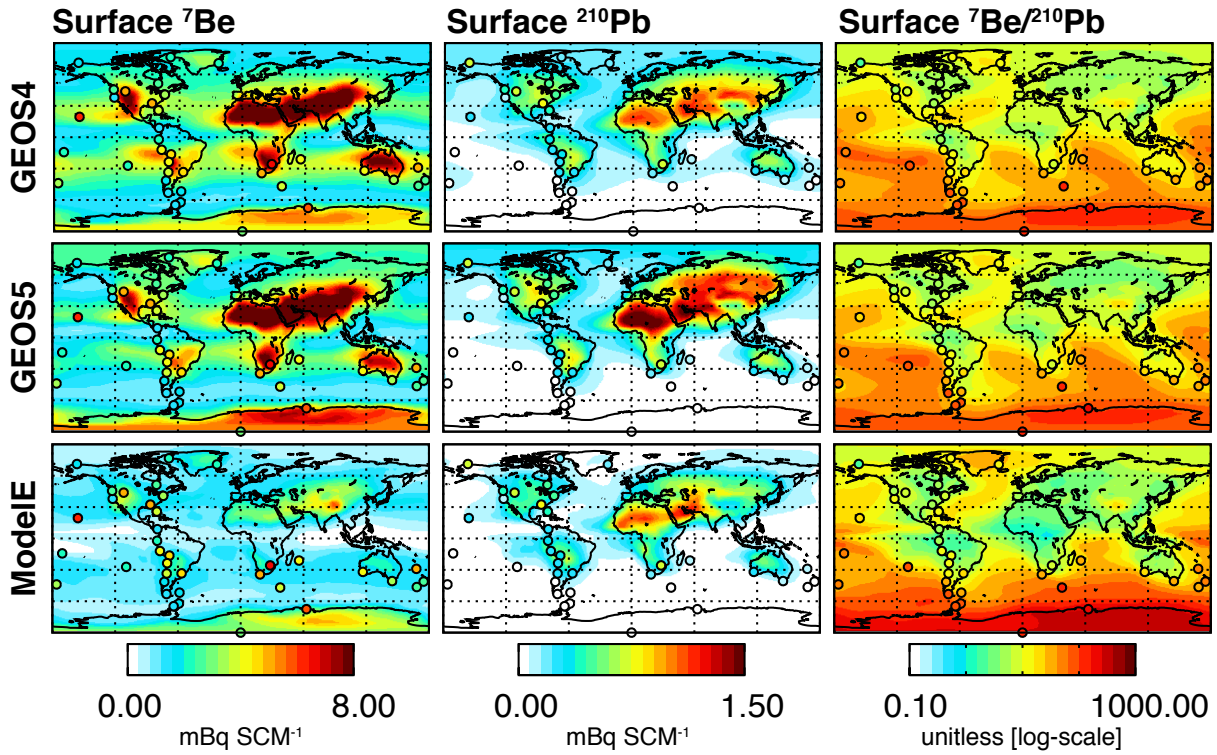

Figure 4: Mean GEOS-Chem surface concentrations of ^{7}Be (left column) and ^{210}Pb (center column), and the ^{7}Be/^{210}Pb ratio (right column). Filled circles show the long-term mean observations from the DOE SASP network. The ^{7}Be observations have been selected for periods of average solar activity.

mental Measurements Laboratory (EML) Surface Air Sampling Program (SASP) (http://www.nbl.doe.gov/htm/EML_Legacy_Website/). SASP recorded the spatial and temporal distribution of various radionuclides in surface ambient air from 1957 until 1999, including ^{7}Be and ^{210}Pb. For comparison with our simulations, we select data from periods of average solar activity (solar modulation potential Φ = 670 $\pm$ 50 MV from the Usoskin et al. (2005) reconstruction). Surface concentrations of both ^{7}Be and ^{210}Pb are lower in the ModelE simulation, consistent with the shorter lifetime against deposition. The ^{7}Be/^{210}Pb ratio is higher in the polar regions and lower in the tropics than in the GEOS simulations, which imply less tropical mixing and more polar vertical mixing in the ModelE simulations.

2.2.2 Stratosphere

Figure 5 shows the simulated zonal distributions of the annual mean age of air in the stratosphere, which is defined as the mean time since air at a particular point in the stratosphere was last in the troposphere (Hall and Waugh, 2000). Age of air increases away from the tropopause and equator, where most tropospheric air enters the stratosphere (Holton et al., 1995). We determine age of air by using SF_6 as a chronological tracer (Waugh and Hall, 2002) to determine the average temporal lag between a concentration at given location in the stratosphere relative to the tropical upper troposphere. We use the period 1995-2012, in which the atmospheric burden of SF_6 grew linearly in our simulations.

Most models underestimate the stratospheric age of air implied by observations of CO_2, SF_6, and HF, which increases up to 7 years by 35 km in the poles (Waugh and Hall, 2002). GEOS-Chem using ModelE is most accurate in reproducing

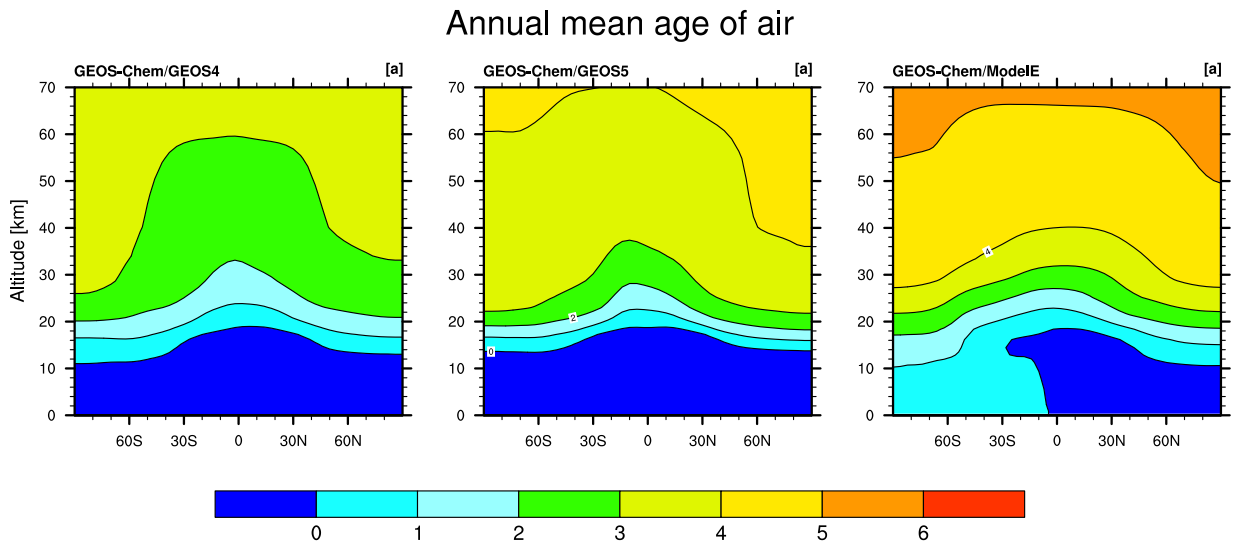

Figure 5: Average age of air in the stratosphere in GEOS-Chem simulations driven by GEOS4, GEOS5 and GISS ModelE, using as a chronological tracer the temporal lag in the simulated 1995-2012 time series of SF_6 relative to the tropical tropopause (Waugh and Hall, 2002).

the average age of air implied from the observations. However, the shallower meridional gradient of ModelE indicates a stronger "leaky pipe" (e.g., Ray et al., 2010) and more poleward flow in the lower tropical stratosphere than in either GEOS model. Coupled with an overly vigorous stratosphere-troposphere exchange (next section), this apparently allows for more efficient transport from the tropical to the Antarctic troposphere via the lower stratosphere, and leads to an overestimate of stratospheric ozone concentrations in the extratropical lower stratosphere.

2.2.3 Stratosphere-Troposphere Exchange

Beryllium-7 has often been used as a tracer of downward transport from the stratosphere (Dibb et al., 1992, 1994; Husain et al., 1977; Rehfeld and Heimann, 1995; Sanak et al., 1985; Viezee and Singh, 1980) and as an indicator of STE performance within global atmospheric models (Allen et al., 2003; Liu et al., 2001, in prep.; Barrett et al., 2012).

Figure 6 shows the annual zonal fraction of ^{7}Be of stratospheric origin in each simulation. Using GEOS4 and GEOS5 meteorology, we find that 24-26% of annual average surface midlatitude concentrations of ^{7}Be is of stratospheric origin, consistent with the Dutkiewicz and Husain (1985) constraint of 25% from ^{7}Be/90Sr for 38-51 N. For ModelE using QUS, we find a slight underestimate of 20-25%. However, the fraction throughout the polar free troposphere in the ModelE-driven simulation is much higher than in the GEOS simulations, implying a larger stratosphere-to-troposphere mass flux. The amount of ^{7}Be over Antarctica in ModelE of stratospheric origin is roughly double that of either GEOS simulation. Our results are similar to the NASA Global Modeling Initiative (GMI) CTM driven by GISS Model II' meteorology (Liu et al., in prep.).

We found that application of the GISS QUS winds to the standard TPCORE advection scheme in GEOS-Chem originally lead to much larger overestimates in stratosphere-troposphere mixing, as small inconsistencies in the the horizontal mass fluxes manifest as large vertical fluxes. This problem was apparent in earlier GEOS-Chem simulations using GISS Model III meteorology, especially at the poles, (e.g., Wu et al., 2007), but as the cross-tropopause flux of

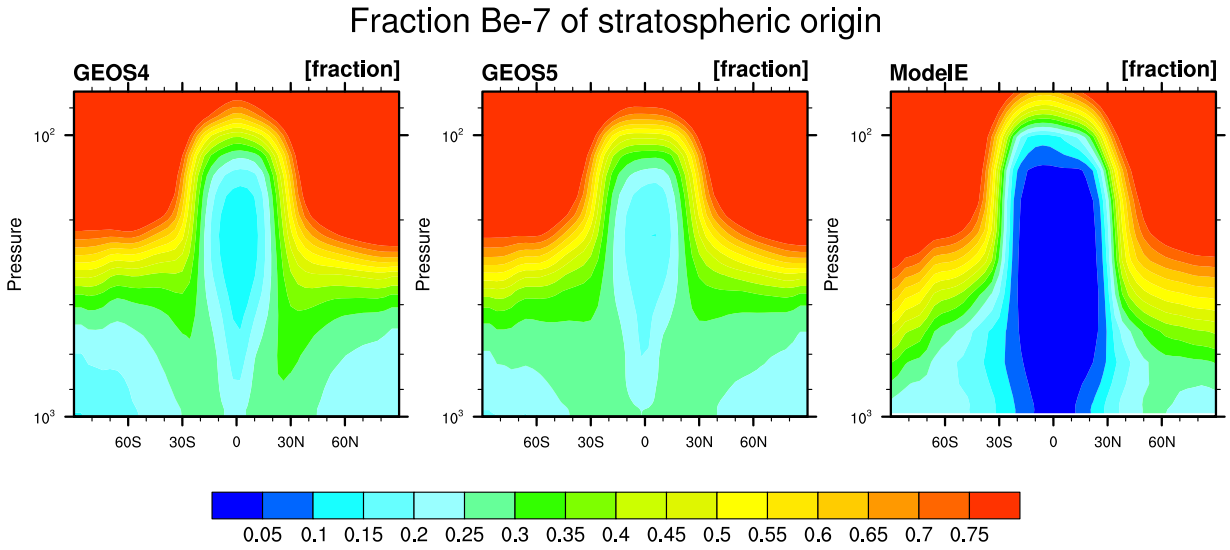

Figure 6: Zonal annual mean fraction ^{7}Be of stratospheric origin in GEOS-Chem driven by different meteorology. Tropopause determined using local lapse rate.

ozone in those simulations was prescribed, it was less of an issue in those studies. To allow for online stratospheric chemistry in this study, we found it necessary to implement the QUS advection scheme within GEOS-Chem.

2.3 Wet Deposition

Figure 7 (right column) compares the mean ^{210}Pb wet deposition flux in each simulation with that of the long-term mean aggregated from rainfall collectors, soil cores, and snow samples by Preiss et al. (1996) aggregated to the model resolutions. GEOS-Chem captures the magnitude and global spatial distribution of the ^{210}Pb deposition flux, with the exception of the East Asian outflow. Wet deposition of ^{210}Pb in the GEOS simulations is biased by -16% and -26%, and by -16% in the ModelE simulation versus the observations. If we neglect the observations over the Japanese archipelago, which may reflect in situ production of ^{210}Pb on mineral dust aerosol (Fukuda and Tsunogai, 1975) that we do not simulate, the GEOS simulations remain similarly biased (-13 to -28%), but ModelE is now positively biased by +7%. Altogether, these results imply a small low bias in the ^{210}Pb source (and therefore ^{222}Rn emission), although the results are clearly sensitive to precipitation distributions.

We find a tropospheric residence time for ^{210}Pb-containing aerosols against deposition in our ModelE-driven simulation of 7.2 d, shorter than than with GEOS4 (9.5 d) or GEOS5 (11 d) meteorology for 2004-2006, but within the range of previous estimates, 6.5-12.5 d (Turekian et al., 1977; Lambert et al., 1982; Balkanski et al., 1993; Koch et al., 1996; Guelle et al., 1998b,a; Liu et al., 2001).

Figure 7 (left column) examines the modeled ^{7}Be wet deposition fluxes, compared against the few available observations (Baskaran et al., 1993; Bleichrodt, 1978; Brown et al., 1989; Dibb, 1989; Du et al., 2008; Harvey and Matthews, 1989; Hasebe et al., 1981; Hirose et al., 2004; Igarashi et al., 1998; Narazaki and Fujitaka, 2010; Nijampurkar and Rao, 1993; Olsen et al., 1985; Papastefanou et al., 1995; Schuler et al., 1991; Turekian et al., 1983; Wallbrink and Murray,

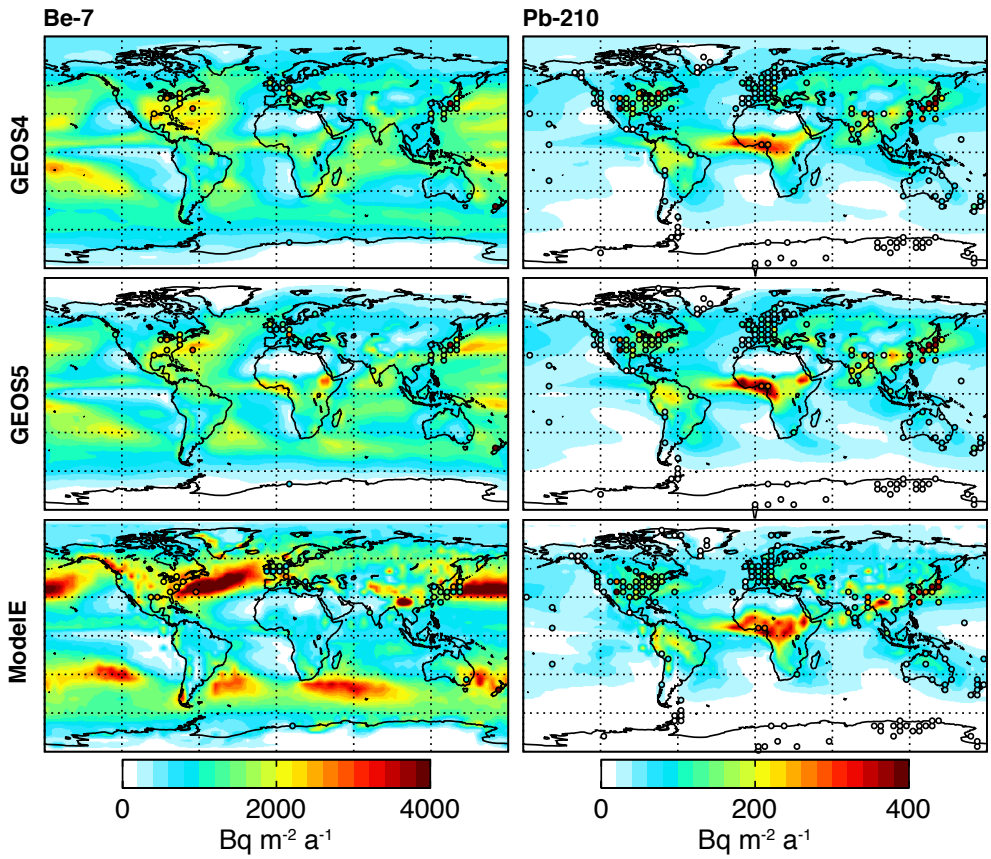

Figure 7: GEOS-Chem annual average aerosol wet deposition flux for ^{7}Be (left column) and ^{210}Pb (right column). Each row uses different meteorology. The filled circles show observed values aggregated to the model resolution.

1994, and references therein). The wet deposition flux is increased in our ModelE simulation relative to the GEOS simulations, particularly over the midlatitude oceans. This result reflects the higher stratosphere-to-troposphere mass flux in ModelE, which increases the fraction of the ^{7}Be burden in the troposphere relative to the stratosphere. It also derives from greater precipitation in regions of stratospheric downwelling, which increases the fraction of ^{7}Be lost by deposition rather than by radioactive decay. Compared to observed values of ^{7}Be, the ModelE-driven simulation shows a bias of +33% while GEOS4 and GEOS5 yield biases of -22% and -26%. The spread in biases shows the difficulty in modeling precipitation accurately, as well as large variability in the observed fluxes induced by the solar cycle.

We find a lifetime of tropospheric ^{7}Be against wet deposition of 40 d in our ModelE simulation, which is consistent with our GEOS5 simulation, and longer than our GEOS4 simulation (32 d). These lifetimes are all longer than prior findings, e.g., 23 d (Koch et al., 1996) and 21 d (Liu et al., 2001), but within the variability expected from the sensitivity of the calculation to model vertical resolution and tropopause definition, as the ^{7}Be burden straddles the tropopause.

2.4 Hydroxyl Radical

To assess OH concentrations in the model, we examine the lifetime and/or distributions of relatively long-lived molecules whose main sink in the troposphere is OH. We find that the lifetime of methyl chloroform (MCF) against tropospheric

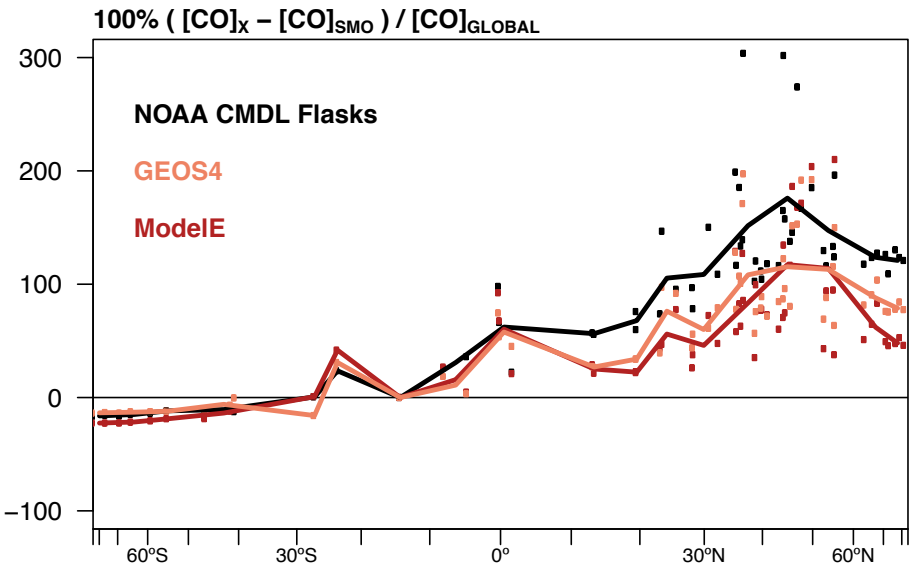

Figure 8: Meridional gradient of CO in flask samples for 1990-2010 at sites in the NOAA Global Monitoring Division, relative to American Samoa (SMO; 14 S). Also shown are the values from GEOS-Chem driven by ModelE and GEOS4 meteorology sampled at the month and location of the observations (filled circles). The solid lines show the mean for 20 latitudinal bins of equal meridional length.

OH is 5.5 years in the CTM driven by present-day meteorology from ModelE, matching recent multi-model estimates of 5.7 $\pm$ 0.9 years (Naik et al., 2013), and close to the observed constraint of $6.0^{+0.5}_{0.4}$ years from Prinn et al. (2005). The simulated methane lifetime against loss by tropospheric OH is 10.4 years, which agrees with the best estimate of $10.2^{+0.9}_{0.7}$ years derived from the MCF data (Prinn et al., 2005), recent multi-model estimates of 10.2 $\pm$ 1.7 (Fiore et al., 2009) and 9.8 $\pm$ 1.6 (Voulgarakis et al., 2013) years, and an estimate of 11.2 $\pm$ 1.3 years derived from methane observations (Prather et al., 2012). The present-day simulation captures the observed meridional gradient of CO in the southern hemisphere. Like most other models (Shindell et al., 2006), our simulations underestimate the CO gradient in the northern hemisphere by about a third, for reasons that are uncertain (Figure 8).

2.5 NO_x

Figure 9 compares tropospheric columns of NO_2 from the GOME satellite to those from the present-day ICECAP simulation. Satellite retrievals of NO_2 are most sensitive to surface NO_x, and are therefore useful for evaluating anthropogenic NO_x sources in models (e.g., van Noije et al., 2006). The model well reproduces the spatial distribution of NO_2 with $R^2 = 0.83$ ($n = 72$ longitudes $\times$ 46 latitudes). The model is lower on average than the GOME product by 29%, which is within the satellite product's range of uncertainty (35-60%; Boersma et al., 2004), and could additionally reflect differences in the tropopause heights used here versus the satellite product (Shindell et al., 2013).

2.6 Ozone

Figure 10a shows that total ozone columns (TOC) over the tropics (30 S-30 N) in the ModelE-driven simulations have a small bias (+1.5%) against 1990-1999 mean TOC from the TOMS/SBUV merged total ozone data set, version 8,

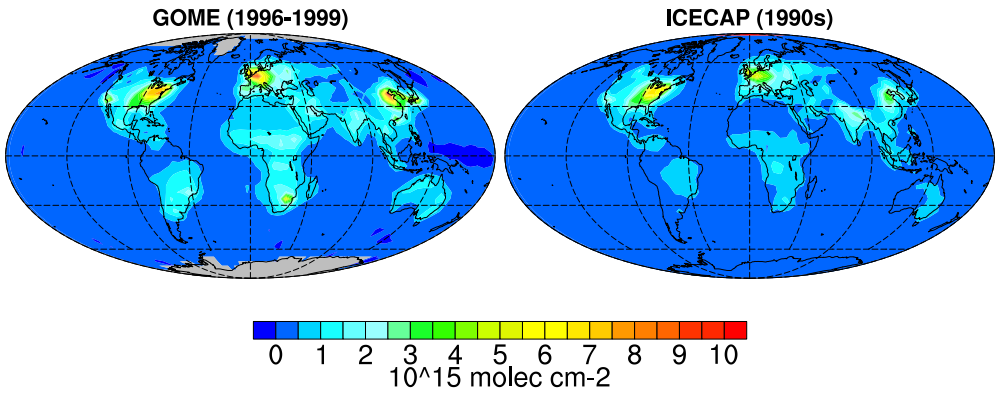

Figure 9: Annual average tropospheric columns of NO_2 from the GOME satellite (left) and in the ICECAP present-day simulation (right). The model is sampled daily at the satellite overpass time (10:30 local time) and integrated up to the model's thermal tropopause for comparison. Negative values in the GOME product occur as it is determined by subtracting simulated stratospheric columns from total column measurements.

revision 3 (available online at http://acd-ext.gsfc.nasa.gov/Data_services/merged/). Data from the Aura satellite allow for isolating the stratospheric and tropospheric contributions to TOC (Ziemke et al., 2011). Figure 10b shows that over the tropics (30 S-30 N), where the stratosphere has its greatest influence on tropospheric photochemistry, the simulated stratospheric columns of ozone (SCO) agree within 5% of the Ziemke et al. (2011) satellite climatology (mean bias ModelE: +0.2%; GEOS4: +4.8%). Extratropical SCO is overestimated by up to 100% in both simulations, particularly over the southern hemisphere, resulting from overly strong meridional air mass fluxes in the lower stratosphere from the tropical regions of net photochemical production (Section S2.2.2 and S2.2.3). Figure 10c shows tropospheric columns of ozone (TCO). ModelE and GEOS4 are biased low by 20% and 9% in the tropics versus the 2000s TCO climatology from OMI/MLS (Ziemke et al., 2006). The overly vigorous stratospheric-troposphere exchange in ModelE leads to a cross-tropopause flux of ozone from the stratosphere that is approximately 40% higher in the CTM driven by ModelE than GEOS4. This causes large overestimates in tropospheric ozone in the extratropics (+46% from 60 S-30 S and +44% from 30 N-60 N), particularly during the spring months. On the other hand, GEOS4 is biased low in the extratropics (-32% from 60 S-30 S and -12% from 30 N-60 N) due to the recent inclusion of bromine chemistry in the model. Figure 11 compares the modeled ozone profiles against all available ozonesondes for the 1990s from the World Ozone and Ultraviolet Radiation Data Center (WOUDC; http://www.woudc.org), using the zonal bands and pressure levels from Stevenson et al. (2006). Most of the tropical bias occurs in the free and upper troposphere, and is within the range of observed variability. GEOS4 is biased low in the extratropics with the recent inclusion of bromine chemistry in the model. The ModelE biases in the extratropics are again consistent with the overestimate of stratosphere-troposphere exchange.

In summary, GEOS-Chem driven by ModelE for the ICECAP project recreates the global lifetimes of MCF and methane against oxidation by tropospheric OH implied by observation (better than GEOS simulations), and has very small bias in its tropical overhead stratospheric ozone columns. Its greatest limitation is in an overly vigorous mass flux from the stratosphere, which creates large biases in extratropical tropospheric ozone. It also underestimates the ozone burden in the tropical upper troposphere. Future projects using the ICECAP framework will increase the horizontal and vertical resolution of the GCM to improve mass transport, and/or the model top pressure (van Velthoven and Kelder,

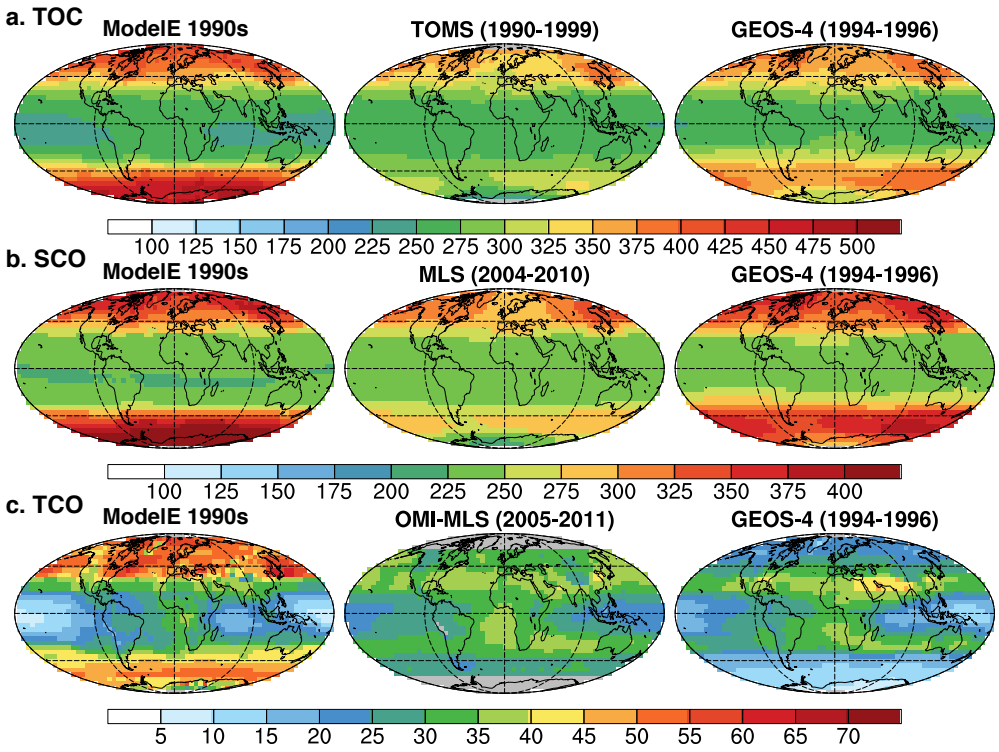

Figure 10: Annual average total ozone columns (TOC; top panel), stratospheric columns of ozone (SCO; middle panel), and tropospheric columns of ozone (TCO; bottom panel). The left column shows ozone columns determined from GEOS-Chem driven by three years of present-day GISS ModelE meteorology. The center column shows satellite climatologies of TOC in the 1990s from the TOMS/SBUV TOMS/SBUV merged data, the 2004-2010 SCO climatology from the Microwave Limb Sounder (MLS) (Ziemke et al., 2011), and the 2005-2011 TCO climatology from OMI/MLS (Ziemke et al., 2006). The right column shows ozone columns in GEOS-Chem driven by GEOS4 meteorology for 1993-1996. All units are Dobson Units (DU). Tropopause determined in the simulations using thermal lapse rate for comparison with satellite stratospheric and tropospheric products.

1996; Austin et al., 1997; Rind et al., 1999).

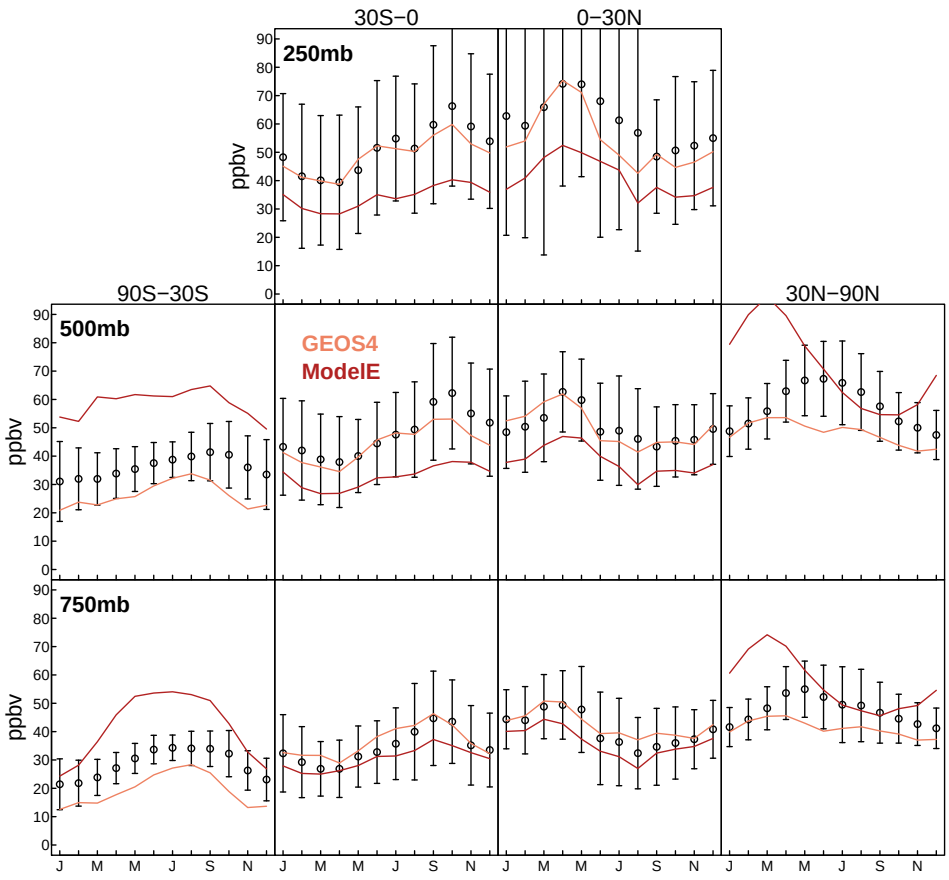

Figure 11: Comparison of the annual cycle of ozone observations (black dots) and model results (colored lines), sampled for different latitude bands (90 S–30 S, 30 S to equator; equator to 30 N, and 30 N–90 N) and different pressure levels (750, 500, and 250 hPa). The models are sampled at the same sites and with the same frequency as the observations. The bars for each observation are the average of the interannual standard deviations at each station.

References

Allen, D. J., Rood, R., Thompson, A. M., and Hudson, R.: Three-dimensional radon 222 calculations using assimilated meteorological data and a convective mixing algorithm, J Geophys Res-Atmos, 101, 6871--6881, 1996.

Allen, D. J., Dibb, J., Ridley, B., Pickering, K., and Talbot, R.: An estimate of the stratospheric contribution to springtime tropospheric ozone maxima using TOPSE measurements and beryllium-7 simulations, J Geophys Res-Atmos, 108, 2003.

Austin, J., Butchart, N., and Swinbank, R.: Sensitivity of ozone and temperature to vertical resolution in a gcm with coupled stratospheric chemistry, Q J Roy Meteor Soc, 123, 1405--1431, 1997.

Balkanski, Y., Jacob, D. J., Gardner, G., Graustein, W., and Turekian, K.: Transport and Residence Times of Tropospheric Aerosols Inferred From a Global 3-Dimensional Simulation of Pb-210, J Geophys Res-Atmos, 98, 20 573--20 586, 1993.

Barrett, S. R. H., Yim, S. H. L., Gilmore, C. K., Murray, L. T., Kuhn, S. R., Tai, A. P. K., Yantosca, R. M., Byun, D. W., Ngan, F., Li, X., Levy, J. I., Ashok, A., Koo, J., Wong, H. M., Dessens, O., Balasubramanian, S., Fleming, G. G., Pearlson, M. N., Wollersheim, C., Malina, R., Arunachalam, S., Binkowski, F. S., Leibensperger, E. M., Jacob, D. J., Hileman, J. I., and Waitz, I. A.: Public Health, Climate, and Economic Impacts of Desulfurizing Jet Fuel, Environ Sci Technol, 46, 4275--4282, 2012.

Baskaran, M., Coleman, C., and Santschi, P.: Atmospheric Depositional Fluxes of Be-7 and Pb-210 at Galveston and College-Station, Texas, J Geophys Res-Atmos, 98, 20 555--20 571, 1993.

Bleichrodt, J.: Mean Tropospheric Residence Time of Cosmic-Ray-Produced Beryllium-7 at North Temperate Latitudes, J Geophys Res-Oc Atm, 83, 3058--3062, 1978.

Boersma, K. F., Eskes, H. J., and Brinksma, E. J.: Error analysis for tropospheric NO2 retrieval from space, Journal of Geophysical Research: Atmospheres (1984--2012), 109, D04 311, 2004.

Bondietti, E., Brantley, J., and Rangarajan, C.: Size Distributions and Growth of Natural and Chernobyl-Derived Sub-Micron Aerosols in Tennessee, J Environ Radioactiv, 6, 99--120, 1988.

Bradley, W. and Pearson, J.: Aircraft Measurements of Vertical Distribution of Radon in Lower Atmosphere, J Geophys Res, 75, 5890, 1970.

Brost, R. and Chatfield, R.: Transport of Radon in a 3-Dimensional, Subhemispheric Model, J Geophys Res-Atmos, 94, 5095--5119, 1989.

Brost, R., Feichter, J., and Heimann, M.: 3-Dimensional Simulation of Be-7 in a Global Climate Model, J Geophys Res-Atmos, 96, 22 423--22 445, 1991.

Brown, L., Stensland, G., Klein, J., and Middleton, R.: Atmospheric Deposition of Be-7 and Be-10, Geochim Cosmochim Ac, 53, 135--142, 1989.

Considine, D., Bergmann, D., and Liu, H.: Sensitivity of Global Modeling Initiative chemistry and transport model simulations of radon-222 and lead-210 to input meteorological data, Atmos Chem Phys, 5, 3389--3406, 2005.

Dibb, J.: Atmospheric Deposition of Beryllium-7 in the Chesapeake Bay Region, J Geophys Res-Atmos, 94, 2261--2265, 1989.

Dibb, J., Talbot, R., and Gregory, G.: Beryllium-7 and Pb-210 in the Western-Hemisphere Arctic Atmosphere - Observations From Three Recent Aircraft-Based Sampling Programs, J Geophys Res-Atmos, 97, 16 709--16 715, 1992.

Dibb, J., Meeker, L., Finkel, R., Southon, J., Caffee, M., and Barrie, L.: Estimation of Stratospheric Input to the Arctic Troposphere - Be-7 and Be-10 in Aerosols at Alert, Canada, J Geophys Res-Atmos, 99, 12 855--12 864, 1994.

Du, J., Zhang, J., Zhang, J., and Wu, Y.: Deposition patterns of atmospheric Be-7 and Pb-210 in coast of East China Sea, Shanghai, China, Atmos Environ, 42, 5101--5109, 2008.

Dutkiewicz, V. and Husain, L.: Stratospheric and Tropospheric Components of Be-7 in Surface Air, J Geophys Res-Atmos, 90, 5783--5788, 1985.

Feichter, J. and Crutzen, P.: Parameterization of vertical tracer transport due to deep cumulus convection in a global transport model and its evaluation with ^{222}Radon measurements, Tellus B, 42, 100--117, 1990.

Fiore, A. M., Dentener, F. J., Wild, O., Cuvelier, C., Schultz, M. G., Hess, P., Textor, C., Schulz, M., Doherty, R. M., Horowitz, L. W., MacKenzie, I. A., Sanderson, M. G., Shindell, D. T., Stevenson, D. S., Szopa, S., Van Dingenen, R., Zeng, G., Atherton, C., Bergmann, D., Bey, I., Carmichael, G., Collins, W. J., Duncan, B. N., Faluvegi, G., Folberth, G., Gauss, M., Gong, S., Hauglustaine, D., Holloway, T., Isaksen, I. S. A., Jacob, D. J., Jonson, J. E., Kaminski, J. W., Keating, T. J., Lupu, A., Marmer, E., Montanaro, V., Park, R. J., Pitari, G., Pringle, K. J., Pyle, J. A., Schroeder, S., Vivanco, M. G., Wind, P., Wojcik, G., Wu, S., and Zuber, A.: Multimodel estimates of intercontinental source-receptor relationships for ozone pollution, J Geophys Res-Atmos, 114, 2009.

Fukuda, K. and Tsunogai, S.: Pb-210 in Precipitation in Japan and Its Implication for Transport of Continental Aerosols Across Ocean, Tellus, 27, 514--521, 1975.

Guelle, W., Balkanski, Y., Dibb, J., Schulz, M., and Dulac, F.: Wet deposition in a global size-dependent aerosol transport model 2. Influence of the scavenging scheme on Pb-210 vertical profiles, surface concentrations, and deposition, J Geophys Res-Atmos, 103, 28 875--28 891, 1998a.

Guelle, W., Balkanski, Y., Schulz, M., Dulac, F., and Monfray, P.: Wet deposition in a global size-dependent aerosol transport model - 1. Comparison of a 1 year Pb-210 simulation with ground measurements, J Geophys Res-Atmos, 103, 11 429--11 445, 1998b.

Hall, B. D., Dutton, G. S., Mondeel, D. J., Nance, J. D., Rigby, M., Butler, J. H., Moore, F. L., Hurst, D. F., and Elkins, J. W.: Improving measurements of SF_6 for the study of atmospheric transport and emissions, Atmos. Meas. Tech., 4, 2441--2451, 2011.

Hall, T. M. and Waugh, D. W.: Stratospheric residence time and its relationship to mean age, J Geophys Res, 105, 6773, 2000.

Harvey, M. and Matthews, K.: Be-7 Deposition in a High-Rainfall Area of New-Zealand, J Atmos Chem, 8, 299--306, 1989.

Hasebe, N., Doke, T., Kikuchi, J., Takeuchi, Y., and Sugiyama, T.: Observation of Fallout Rates of Atmospheric Be-7 and Na-22 Produced by Cosmic-Rays Concerning Estimation of the Fallout Rate of Atmospheric Al-26, J Geophys Res-Space, 86, 520--524, 1981.

Hauglustaine, D., Hourdin, F., Jourdain, L., Filiberti, M., Walters, S., Lamarque, J., and Holland, E.: Interactive chemistry in the Laboratoire de Meteorologie Dynamique general circulation model: Description and background tropospheric chemistry evaluation, J Geophys Res-Atmos, 109, 2004.

Hirose, K., Honda, T., Yagishita, S., Igarashi, Y., and Aoyama, M.: Deposition behaviors of Pb-210, Be-7 and thorium isotopes observed in Tsukuba and Nagasaki, Japan, Atmos Environ, 38, 6601--6608, 2004.

Holton, J., Haynes, P., Mcintyre, M., Douglass, A., Rood, R., and Pfister, L.: Stratosphere-Troposphere Exchange, Rev Geophys, 33, 403--439, 1995.

Husain, L., Coffey, P., Meyers, R., and Cederwall, R.: Ozone Transport From Stratosphere to Troposphere, Geophys Res Lett, 4, 363--365, 1977.

Igarashi, Y., Hirose, I., and Otsuji-Hatori, M.: Beryllium-7 deposition and its relation to sulfate deposition, J Atmos Chem, 29, 217--231, 1998.

Jacob, D. J.: Radon-222 as a test of convective transport in a general circulation model, Tellus B, 42, 118--134, 1990.

Jacob, D. J., Prather, M., Rasch, P., Shia, R., Balkanski, Y., Beagley, S., Bergmann, D., Blackshear, W., Brown, M., Chiba, M., Chipperfield, M., deGrandpre, J., Dignon, J., Feichter, J., Genthon, C., Grose, W., Kasibhatla, P., Kohler, I., Kritz, M., Law, K., Penner, J. E., Ramonet, M., Reeves, C., Rotman, D., Stockwell, D., VanVelthoven, P., Verver, G., Wild, O., Yang, H., and Zimmermann, P.: Evaluation and intercomparison of global atmospheric transport models using Rn-222 and other short-lived tracers, J Geophys Res-Atmos, 102, 5953--5970, 1997.

Koch, D., Jacob, D. J., and Graustein, W.: Vertical transport of tropospheric aerosols as indicated by Be-7 and Pb-210 in a chemical tracer model, J Geophys Res-Atmos, 101, 18 651--18 666, 1996.

Kritz, M., Rosner, S., and Stockwell, D.: Validation of an off-line three-dimensional chemical transport model using observed radon profiles - 1. Observations, J Geophys Res-Atmos, 103, 8425--8432, 1998.

Lal, D., Malhotra, P., and Peters, B.: On the Production of Radioisotopes in the Atmosphere by Cosmic Radiation and Their Application to Meteorology, J Atmos Terr Phys, 12, 306--328, 1958.

Lambert, G., Polian, G., Sanak, J., Ardouin, B., Buisson, A., Jegou, A., and Leroulley, J.: Cycle du radon et de ses descendants: application à l'étude des échanges troposphère-stratosphère, Ann Geophys, 38, 497--531, 1982.

Liu, H., Jacob, D. J., Bey, I., and Yantosca, R.: Constraints from Pb-210 and Be-7 on wet deposition and transport in a global three-dimensional chemical tracer model driven by assimilated meteorological fields, J Geophys Res-Atmos, 106, 12 109--12 128, 2001.

Liu, H., Considine, D. B., Horowitz, L. W., Crawford, J. H., Strahan, S. E., Damon, M., Rodriguez, J. M., Xu, X., Carouge, C. C., and Yantosca, R. M.: Using beryllium-7 to assess cross-tropopause transport in global models, in prep.

Maenhaut, W., Zoller, W., and Coles, D.: Radionuclides in the South Pole Atmosphere, J Geophys Res-Oc Atm, 84, 3131--3138, 1979.

Mahowald, N., Rasch, P., and Prinn, R.: Cumulus parameterizations in chemical transport models, J Geophys Res-Atmos, 100, 26 173--26 189, 1995.

Maiss, M. and Brenninkmeijer, C. A. M.: Atmospheric SF 6: Trends, Sources, and Prospects, Environ Sci Technol, 32, 3077--3086, 1998.

Moore, H., Poet, S., and Martell, E.: Rn-222, Pb-210, Bi-210, and Po-210 Profiles and Aerosol Residence Times Versus Altitude, J Geophys Res, 78, 7065--7075, 1973.

Naik, V., Voulgarakis, A., Fiore, A. M., Horowitz, L. W., Lamarque, J. F., Lin, M., Prather, M. J., Young, P. J., Bergmann, D., Cameron-Smith, P. J., Cionni, I., Collins, W. J., Dalsøren, S. B., Doherty, R., Eyring, V., Faluvegi, G., Folberth, G. A., Josse, B., Lee, Y. H., MacKenzie, I. A., Nagashima, T., van Noije, T. P. C., Plummer, D. A., Righi, M., Rumbold, S. T., Skeie, R., Shindell, D. T., Stevenson, D. S., Strode, S., Sudo, K., Szopa, S., and Zeng, G.: Preindustrial to present-day changes in tropospheric hydroxyl radical and methane lifetime from the Atmospheric Chemistry and Climate Model Intercomparison Project (ACCMIP), Atmos Chem Phys, 13, 5277--5298, 2013.

Narazaki, Y. and Fujitaka, K.: The Geographical Distribution and Features of 7Be Deposition in Japan, Japan Health Physics Society, 37, 317--324, 2010.

Nazarov, L., Kuzenkov, A., Malakhov, S., Volokitina, L., Gaziyev, Y., and Vasilyev, A.: Radioactive Aerosol Distribution in Middle and Upper Troposphere Over Ussr in 1963-1968, J Geophys Res, 75, 3575, 1970.

Nijampurkar, V. and Rao, D.: Polar Fallout of Radionuclides Si-32, Be-7 and Pb-210 and Past Accumulation Rate of Ice at Indian Station, Dakshin Gangotri, East Antarctica, J Environ Radioactiv, 21, 107--117, 1993.

Olsen, C., Larsen, I., Lowry, P., Cutshall, N., Todd, J., Wong, G., and Casey, W.: Atmospheric Fluxes and Marsh-Soil Inventories of Be-7 and Pb-210, J Geophys Res-Atmos, 90, 10 487--10 495, 1985.

Papastefanou, C.: Beryllium-7 Aerosols in Ambient Air, Aerosol Air Qual Res, 9, 187--197, 2009.

Papastefanou, C. and Ioannidou, A.: Beryllium-7 aerosols in ambient air, in: Environ Int, pp. S125--S130, 1996.

Papastefanou, C., Ioannidou, A., Stoulos, S., and Manolopoulou, M.: Atmospheric Deposition of Cosmogenic Be-7 and Cs-137 From Fallout of the Chernobyl Accident, Sci Total Environ, 170, 151--156, 1995.

Prather, M. J., Holmes, C. D., and Hsu, J.: Reactive greenhouse gas scenarios: Systematic exploration of uncertainties and the role of atmospheric chemistry, Geophys Res Lett, 39, L09 803, 2012.

Preiss, N., Melieres, M., and Pourchet, M.: A compilation of data on lead 210 concentration in surface air and fluxes at the air-surface and water-sediment interfaces, J Geophys Res-Atmos, 101, 28 847--28 862, 1996.

Prinn, R., Huang, J., Weiss, R., Cunnold, D., Fraser, P., Simmonds, P., McCulloch, A., Harth, C., Reimann, S., Salameh, P., O'Doherty, S., Wang, R., Porter, L., Miller, B., and Krummel, P.: Evidence for variability of atmospheric hydroxyl radicals over the past quarter century, Geophys Res Lett, 32, 2005.

Ray, E. A., Moore, F. L., Rosenlof, K. H., Davis, S. M., Boenisch, H., Morgenstern, O., Smale, D., Rozanov, E., Hegglin, M., Pitari, G., Mancini, E., Braesicke, P., Butchart, N., Hardiman, S., Li, F., Shibata, K., and Plummer, D. A.: Evidence for changes in stratospheric transport and mixing over the past three decades based on multiple data sets and tropical leaky pipe analysis, J Geophys Res, 115, D21 304, 2010.

Rehfeld, S. and Heimann, M.: Three dimensional atmospheric transport simulation of the radioactive tracers Pb-210, Be-7, Be-10, and Sr-90, J Geophys Res-Atmos, 100, 26 141--26 161, 1995.

Rigby, M., Mühle, J., Miller, B. R., Prinn, R. G., Krummel, P. B., Steele, L. P., Fraser, P. J., Salameh, P. K., Harth, C. M., Weiss, R. F., Greally, B. R., O'Doherty, S., Simmonds, P. G., Vollmer, M. K., Reimann, S., Kim, J., Kim, K. R., Wang, H. J., Olivier, J. G. J., Dlugokencky, E. J., Dutton, G. S., Hall, B. D., and Elkins, J. W.: History of atmospheric SF_6 from 1973 to 2008, Atmos Chem Phys, 10, 10 305--10 320, 2010.

Rind, D., Lerner, J., Shah, K., and Suozzo, R.: Use of on-line tracers as a diagnostic tool in general circulation model development: 2. Transport between the troposphere and stratosphere, J Geophys Res-Atmos, 104, 9151--9167, 1999.

Sanak, J., Gaudry, A., and Lambert, G.: Size Distribution of Pb-210 Aerosols Over Oceans, Geophys Res Lett, 8, 1067--1069, 1981.

Sanak, J., Lambert, G., and Ardouin, B.: Measurement of Stratosphere-to-Troposphere Exchange in Antarctica by Using Short-Lived Cosmonuclides, Tellus B, 37, 109--115, 1985.

Schuler, C., Wieland, E., Santschi, P., Sturm, M., Lueck, A., Bollhalder, S., Beer, J., Bonani, G., Hofmann, H., Suter, M., and Wolfli, W.: A Multitracer Studyof Radionuclides in Lake Zurich, Switzerland .1. Comparison of Atmospheric and Sedimentary Fluxes of Be-7, Be-10, Pb-210, Po-210, and Cs-137, J Geophys Res-Oceans, 96, 17 051--17 065, 1991.

Shindell, D. T., Faluvegi, G., Stevenson, D. S., Krol, M. C., Emmons, L. K., Lamarque, J. F., Petron, G., Dentener, F. J., Ellingsen, K., Schultz, M. G., Wild, O., Amann, M., Atherton, C. S., Bergmann, D. J., Bey, I., Butler, T., Cofala, J., Collins, W. J., Derwent, R. G., Doherty, R. M., Drevet, J., Eskes, H. J., Fiore, A. M., Gauss, M., Hauglustaine, D. A., Horowitz, L. W., Isaksen, I. S. A., Lawrence, M. G., Montanaro, V., Mueller, J. F., Pitari, G., Prather, M. J., Pyle, J. A., Rast, S., Rodriguez, J. M., Sanderson, M. G., Savage, N. H., Strahan, S. E., Sudo, K., Szopa, S., Unger, N., van Noije, T. P. C., and Zeng, G.: Multimodel simulations of carbon monoxide: Comparison with observations and projected near-future changes, J Geophys Res-Atmos, 111, 2006.

Shindell, D. T., Pechony, O., Voulgarakis, A., Faluvegi, G., Nazarenko, L., Lamarque, J. F., Bowman, K., Milly, G., Kovari, B., Ruedy, R., and Schmidt, G. A.: Interactive ozone and methane chemistry in GISS-E2 historical and future climate simulations, Atmos Chem Phys, 13, 2653--2689, 2013.

Stevenson, D., Dentener, F., Schultz, M., Ellingsen, K., van Noije, T., Wild, O., Zeng, G., Amann, M., Atherton, C., Bell, N., Bergmann, D., Bey, I., Butler, T., Cofala, J., Collins, W., Derwent, R., Doherty, R., Drevet, J., Eskes, H., Fiore, A., Gauss, M., Hauglustaine, D., Horowitz, L., Isaksen, I., Krol, M., Lamarque, J., Lawrence, M., Montanaro, V., Muller, J., Pitari, G., Prather, M., Pyle, J., Rast, S., Rodriguez, J., Sanderson, M., Savage, N., Shindell, D. T., Strahan, S., Sudo, K., and Szopa, S.: Multimodel ensemble simulations of present-day and near-future tropospheric ozone, J Geophys Res-Atmos, 111, 2006.

Stockwell, D., Kritz, M., Chipperfield, M., and Pyle, J.: Validation of an off-line three-dimensional chemical transport model using observed radon profiles - 2. Model results, J Geophys Res-Atmos, 103, 8433--8445, 1998.

Turekian, K., Nozaki, Y., and Benninger, L.: Geochemistry of Atmospheric Radon and Radon Products, Annu Rev Earth Planet Sci, 5, 227--255, 1977.

Turekian, K., Benninger, L., and Dion, E.: Be-7 and Pb-210 Total Deposition Fluxes at New-Haven, Connecticut and at Bermuda, J Geophys Res-Oc Atm, 88, 5411--5415, 1983.

Usoskin, I., Alanko-Huotari, K., Kovaltsov, G., and Mursula, K.: Heliospheric modulation of cosmic rays: Monthly reconstruction for 1951-2004, J Geophys Res-Space, 110, 2005.

Usoskin, I. G. and Kovaltsov, G. A.: Production of cosmogenic Be-7 isotope in the atmosphere: Full 3-D modeling, J Geophys Res-Atmos, 113, 2008.

van Noije, T. P. C., Eskes, H. J., Dentener, F. J., Stevenson, D. S., Ellingsen, K., Schultz, M. G., Wild, O., Amann, M., Atherton, C. S., Bergmann, D. J., Bey, I., Boersma, K. F., Butler, T., Cofala, J., Drevet, J., Fiore, A. M., Gauss, M., Hauglustaine, D. A., Horowitz, L. W., Isaksen, I. S. A., Krol, M. C., Lamarque, J. F., Lawrence, M. G., Martin, R. V., Montanaro, V., Muller, J.-F., Pitari, G., Prather, M. J., Pyle, J. A., Richter, A., Rodriguez, J. M., Savage, N. H., Strahan, S. E., Sudo, K., Szopa, S., and Roozendael, M. v.: Multi-model ensemble simulations of tropospheric NO$_2$ compared with GOME retrievals for the year 2000, Atmos Chem Phys, 6, 2943--2979, 2006.

van Velthoven, P. F. J. and Kelder, H.: Estimates of stratosphere-troposphere exchange: Sensitivity to model formulation and horizontal resolution, J Geophys Res, 101, 1429, 1996.

Viezee, W. and Singh, H.: The Distribution of Beryllium-7 in the Troposphere - Implications on Stratospheric-Tropospheric Air Exchange, Geophys Res Lett, 7, 805--808, 1980.

Voulgarakis, A., Naik, V., Lamarque, J. F., Shindell, D. T., Young, P. J., Prather, M. J., Wild, O., Field, R. D., Bergmann, D., Cameron-Smith, P., Cionni, I., Collins, W. J., Dalsøren, S. B., Doherty, R. M., Eyring, V., Faluvegi, G., Folberth, G. A., Horowitz, L. W., Josse, B., MacKenzie, I. A., Nagashima, T., Plummer, D. A., Righi, M., Rumbold, S. T., Stevenson, D. S., Strode, S. A., Sudo, K., Szopa, S., and Zeng, G.: Analysis of present day and future OH and methane lifetime in the ACCMIP simulations, Atmos Chem Phys, 13, 2563--2587, 2013.

Wallbrink, P. and Murray, A.: Fallout of Be-7 in South Eastern Australia, J Environ Radioactiv, 25, 213--228, 1994.

Waugh, D. W. and Hall, T. M.: Age of stratospheric air: Theory, observations, and models, Rev Geophys, 40, 1010, 2002.

Wilkening, M.: Rn-222 Concentrations in Convective Patterns of a Mountain Environment, J Geophys Res, 75, 1733, 1970.

Wu, S., Mickley, L. J., Jacob, D. J., Logan, J. A., Yantosca, R. M., and Rind, D.: Why are there large differences between models in global budgets of tropospheric ozone?, J Geophys Res-Atmos, 112, 2007.

Ziemke, J. R., Chandra, S., Duncan, B. N., Froidevaux, L., Bhartia, P. K., Levelt, P. F., and Waters, J. W.: Tropospheric ozone determined from aura OMI and MLS: Evaluation of measurements and comparison with the Global Modeling Initiative's Chemical Transport Model, J Geophys Res-Atmos, 111, 2006.

Ziemke, J. R., Chandra, S., Labow, G. J., Bhartia, P. K., Froidevaux, L., and Witte, J. C.: A global climatology of tropospheric and stratospheric ozone derived from Aura OMI and MLS measurements, Atmos Chem Phys, 11, 9237--9251, 2011.